ACCRETION OF A SATELLITE ONTO A SPHERICAL GALAXY
II. BINARY EVOLUTION AND ORBITAL DECAY

Monica COLPI

Dipartimento di Fisica, Università Degli Studi di Milano, Milano, Italy

ABSTRACT

We study the dynamical evolution of a satellite (of mass M) orbiting around a companion spherical galaxy. The satellite is subject to a back-reaction force $\mathbf{F}_\Delta$ resulting from the density fluctuations excited in the primary stellar system. We evaluate this force using the *linear response theory* developed in Colpi and Pallavicini (1997). $\mathbf{F}_\Delta$ is computed in the reference frame comoving with the primary galaxy and is expanded in multipoles. To lowest order, the force depends on a time integral involving a dynamical 4-point correlation function of the unperturbed background. The equilibrium stellar system (of mass Nm) is described in terms of a Gaussian one-particle distribution function. To capture the relevant features of the physical process determining the evolution of the detached binary, we introduce in the Hamiltonian the harmonic potential as interaction potential among stars. The evolution of the composite system is derived solving for a set of ordinary differential equations; the dynamics of the satellite and of the stars is computed self-consistently.

We determine the conditions for tidal capture of a satellite from an asymptotic free state and give an estimate of the maximum kinetic energy above which encounters do not end in a merger, as a function of the mass ratio M/Nm. We find that capture always leads to final coalescence.

If the binary forms as a bound pair, stability against orbital decay is lost if the pericentric distance is smaller than a critical value. This instability is interpreted in terms of a *near resonance* condition and establishes when the orbital Keplerian frequency becomes comparable to the internal frequency ω of the stellar system.

We show that before coalescence eccentric orbits become progressively less eccentric: The circularization is explored as a function of mass ratio. The time scale of binary coalescence τ_b is a sensitive function of the eccentricity e, for a fixed semimajor axis a and M/Nm ratio: the mismatch between τ_b at $e \sim 0$ and τ_b at $e \sim 1$ can be very large; typically $\tau_b(e \lesssim 1) \sim 6\,\omega^{-1}$, and the time ratio $\tau_b(0)/\tau_b(1) \gtrsim 5$ (for $M/Nm = 0.05$). In addition we find that τ_b obeys a scaling relation with M/Nm, for circular orbits: $\tau_b \propto (M/Nm)^{-\alpha}$ with $\alpha \sim 0.4$. In grazing encounters τ_b is nearly independent of mass.

In a comparison with Weinberg's perturbative technique we demonstrate quantitatively that pinning the center of mass of the galaxy would induce a much larger torque on the satellite.

Subject headings: galaxies: clustering – stars: stellar dynamics

I. INTRODUCTION

In Colpi & Pallavicini (paper I hereafter) it was shown that a satellite moving through a nonuniform stellar background at high speed experiences in addition to *friction* a force that originates from the global *tidal* deformation induced by the satellite in the spherical stellar system during its passage. When the massive object orbits *outside* the companion galaxy, only the tidal component of the force affects its motion: In the high speed limit, this force acting along the instantaneous position $\mathbf{R}$ and along the velocity vector $\mathbf{V}$ induces energy and angular momentum losses.

The results presented in paper I however restrict to the case of shortlived encounters. In such flybys, the typical interaction timescale is much shorter than the dynamical time of the stellar system and this justifies the assumption of uniform motion adopted for the satellite and for the unperturbed trajectories of the stars. In this paper we move a step forward extending our analysis to the study of the orbital evolution of

a binary system composed of a satellite and a spherical galaxy. In the computation of the force, the periodic nature of the satellite orbit is included self-consistently. The force on M, as discussed in paper I, rises from the response of the stellar background to the perturbation induced by the satellite itself and depends on a correlation tensor involving the equilibrium stellar dynamics. As the time scale of the encounter exceeds the dynamical time of the stars bound to the galaxy, we account for the self-gravity of the equilibrium system but neglect the self-gravity of the response (see paper I for details). The binary can become unstable to coalescence as energy can be exchanged between the two members through a complex mechanism involving resonances (Lynden-bell & Kalnajs 1972; Tremaine & Weinberg 1984).

The evolution of a binary can proceed in two phases: in the early phase, the satellite orbits the companion galaxy while progressively losing energy; the binary is detached. In the second more advanced phase, the satellite accretes onto the stellar system: Moving inside the stellar background, it experiences extensive energy losses by dynamical friction, spiraling toward the center of the galaxy.

The *linear response theory* (TLR hereafter) developed in paper I is an ideal tool for exploring the early phase of the dynamical evolution of a satellite in the binary system. It is the aim of the paper to determine under what conditions a binary loses its stability against coalescence and how the evolution develops as a function of the mass of the satellite and of the orbital parameters. This analysis complements and extends an early work by Bontekoe and Van Albada (1987) who explored the orbital decay of a "detached" binary using a numerical simulation. They followed the evolution of a (softened) satellite moving on a close circular orbit around a spherical system (modelled as a polytrope), and found that decay occurs as orbital energy is transferred into internal energy of the primary galaxy that expands thereafter. A numerical simulation was also performed to study evolution in grazing encounters: A satellite moving on an eccentric orbit with pericenter internal to the stellar system was seen to decay towards the companion after a number of revolutions. Here friction intervenes during pericenter passage to cause decay and progressive circularization of the orbit.

A number of problems are still unanswered concerning the nature of the interaction between the extended primary and the satellite. (a) Does the interaction always end in a merger ? (b) When orbital stability is lost, how does evolution proceed ? (c) How does the decay time depend on the initial eccentricity and mass ratio between the satellite and the primary ?

In the "accretion" of a satellite onto the massive companion the longest phase of evolution is the early phase during which the two members are not in physical contact. Due to the weakness of the back-reaction force the evolution is secular, and the system can evolve along a sequence of quasi static states in which the orbital parameters modify. Circularization preceeding infall into the system provides an example of the consequences of the long term evolution (Bontekoe & Van Albada 1987).

These issues are of importance in scenarios for the formation of cosmic structures. Lacey & Cole (1997) recognized the importance played by the values of the orbital parameters in affecting the evolution of baryonic cores in merging halos. Deriving a simplified formula for the merging time scale in the case of a satellite moving inside a singular isothermal halo (using the Chandrasekhar expression for dynamical friction) they showed that the accretion rate of baryonic cores can be significantly lower than the rate of accretion of the dark matter halos themselves if satellites fall preferentially along circular orbits. Thus circularization preceeding the contact phase in a binary can affect the evolution of structures in hierarchical model of galaxy formation (see also Navarro, Frank & White 1994, 1995).

Cosmological N-body simulations of the rise and fall of satellites in galaxy clusters (Tormen 1997) have also shown that satellites accrete onto the primary halo preferentially along orbits of mean circularity ~ 0.5. Lighter satellites are also found to fall on less eccentric orbits compared to the more massive ones which merge from nearly radial orbits. Since the details of the "accretion" process can leave an imprint onto the global shape of the cluster, this calls for a thorough analysis of the underlying physical mechanisms.

Numerical simulations are indeed a viable technique for exploring the evolution over times comparable to a few dynamical times of the primary. However, accretion of light satellites is a secular process and spurious relaxation effect can alter the outcome of numerical runs. The process of orbital decay needs to be explored using alternative methods, and TLR provides a framework for addressing these problems. The method overcomes the difficulty encountered in previous studies (Lin & Tremaine 1983) in which the galaxy was pinned to a fixed center of symmetry and applies to the case of a satellite moving outside the stellar distribution. We describe the process in the frame comoving with the primary and study the early evolution

of the relative orbit.

The outline of the paper is as follows: In §2 we compute the equation of motion of the satellite, within TLR, expanding the force in multipoles. We show that the force can be expressed in terms of a suitable correlation function. In §3 we specify the Hamiltonian of the spherical galaxy in its unperturbed state. The harmonic potential is introduced to describe the interaction potential of the system. This is an idealized model in which the stellar motion is characterized by a unique frequency ω. In this potential we can evaluate the back-reaction force on M self-consistently, i.e., calculating its value on the actual dynamics of the satellite. A binary system can form through capture of the satellite from an asymptotic state, or can come into existence as a bound pair. In §4 we establish the conditions for capture from an initially hyperbolic orbit. In §5 we explore the orbital evolution of a bound pair. We show that orbital decay occurs only it the pericenter distance is smaller than a critical value and we interpret the result in term of a *near* resonant mechanism of energy exchange (§5.2), examining the evolution of circular orbits. The secular torque for a pinned galaxy is computed in §5.3 for a comparison with Weinberg formalism. In §6 we then explore the dependence of the time scale of orbital decay on the initial eccentricity, showing that a large mismatch in the scale exists between circular and very eccentric orbits. The dependence on the mass ratio of the binary members is studied in §6.2 In §7 we present our conclusions.

II. BACK-REACTION FORCE

Consider the case of a satellite of mass M moving in the gravitational field of the primary system consisting of N stars of mass m. In the frame of reference comoving with the center of mass of the stellar distribution the equation of motion for the satellite is

$$\mu \frac{d^2\mathbf{R}(t)}{dt^2} = -GMNm\frac{\mathbf{R}(t)}{|\mathbf{R}(t)|^3} + \mathbf{F}_\Delta \tag{1}$$

where $\mathbf{R}(t)$ is the position vector at time t (relative to this frame) and μ is the reduced mass $\mu = MNm/(Nm+M)$. The force

$$\begin{aligned}\mathbf{F}_\Delta(t) =& [GM]^2 Nm \int_{-\infty}^{t} ds \\ & \int d_3\mathbf{r}\, d_3\mathbf{v}\ \nabla_{\mathbf{v}} f^{\rm op} \cdot \left[\frac{\mathbf{R}(s)-\mathbf{r}}{|\mathbf{R}(s)-\mathbf{r}|^3} - \frac{\mathbf{R}(s)}{|\mathbf{R}(s)|^3}\right]\ \frac{\mathbf{R}(t)-\mathbf{r}(t-s)}{|\mathbf{R}(t)-\mathbf{r}(t-s)|^3}\end{aligned} \tag{2}$$

rises in response to the perturbation induced by the satellite on the spherical system characterized by the one-particle distribution function $f^{\rm op}$ which is isotropic and independent of time: $f^{\rm op}(\mathbf{r},\mathbf{v})$ describes the equilibrium properties of the collisionless stellar system. The expression (2) of the force is equivalent to equation (16b) of paper I modified to account for the motion of the stellar barycenter according to equation (32); it is here derived, using Gauss theorem, in the hypothesis that the motion of the satellite is *external* to the companion galaxy.

The force depends on the past history of the satellite and on the response of the stellar system: $\mathbf{r}(s)$ and $\mathbf{v}(s)$ denote the position and velocity vectors of the stars at time s as determined by the equilibrium Hamiltonian H_0. In equation (2) the perturbation vanishes as $t \to -\infty$.

Since the satellite distance R exceeds the stellar mean radius $< r^2 >^{1/2}$ we can expand the force in multipoles. We thus evaluate $\mathbf{F}_\Delta$ expanding in series the terms of the form

$$\frac{R^a - r^a}{|\mathbf{R}-\mathbf{r}|^3} = \frac{R^a}{R^3} + Q^{ab}r^b + \frac{1}{2}O^{abc}r^b r^c \tag{3}$$

where

$$Q^{ab} \equiv \frac{3R^aR^b - \delta^{ab}R^2}{R^5} \tag{4}$$

and

$$O^{abc} \equiv -\frac{3}{R^5}(\delta^{ab}R^c + \delta^{ac}R^b + \delta^{cb}R^a) + \frac{15}{R^7}R^aR^bR^c. \tag{5}$$

In equation (2) the monopole terms in squared brackets cancel out identically. In addition, because of the isotropy of the distribution function in the velocity space, and of the symmetry of equation (2) in the exchange between $\mathbf{r} \to -\mathbf{r}$ and $\mathbf{v} \to -\mathbf{v}$ yielding $\mathbf{r}(t-s) \to -\mathbf{r}(t-s)$, we find that the leading terms are only those coupling a quadrupole term ($\propto Q^{ab}r^b$) with a octupole term ($\propto O^{abc}r^br^c$).

If we include the explicit expression of the quadrupole and octupole terms in equation (2) we find that the force $\mathbf{F}_\Delta$ on M depends simply on the dynamics of the particles (in their unperturbed state) through correlation tensors of the form

$$< v^a r^b\, r^c(t-s)\, r^d(t-s) > \qquad \text{or} \qquad < v^a r^b\, r^c\, r^d(t-s) > \tag{6}$$

where the components of $\mathbf{v}$ and $\mathbf{r}$ are referred at current time t, and $\mathbf{r}(t-s)$ at time $(t-s)$.

Because of the isotropy of the unperturbed stellar distribution function the tensors depend only on four scalar functions which we introduce as follows:

$$< v^a\, r^b\, r^c(t-s)\, r^d(t-s) >= \delta^{ab}\delta^{cd}\mathcal{A}(t-s) + (\delta^{ac}\delta^{bd} + \delta^{ad}\delta^{bc})\mathcal{B}(t-s) \tag{7}$$

$$< v^a\, r^b\, r^c\, r^d(t-s) >= \delta^{ad}\delta^{cd}\mathcal{C}(t-s) + (\delta^{ab}\delta^{cd} + \delta^{ac}\delta^{bd})\mathcal{D}(t-s) \tag{8}$$

where δ is the Kronecher symbol and $<>$ denotes the mean over the equilibrium distribution function $f^{\rm op}$.

If equations (7-8) are inserted in (2) we find that the back-reaction force $\mathbf{F}_\Delta$ depends only on the correlation function $\mathcal{B}$ and reads

$$F^a_\Delta(t) = -[GM]^2\, N\, m^2 \beta O^{abc}(t) \int_{-\infty}^{t} ds\ \mathcal{B}(t-s) Q^{bc}(s) \tag{9}$$

where the tensor O is evaluated at the actual position of the satellite, i.e., at time t, and Q at the earlier time s depending on $R(s)$. In deriving equation (9) we have introduced the assumption that $f^{\rm op}$ is Gaussian in the velocity space: Accordingly, $\nabla_{\mathbf{v}} f^{\rm op} = -\beta\, m f^{\rm op}$, where the coefficient $\beta \equiv (m\sigma^2)^{-1}$, is a function of σ denoting the one-dimensional stellar dispersion velocity (see Paper I). We will refer to $\mathbf{F}_\Delta$ as back-reaction or tidal force, hereafter.

We find that to leading order in the multipole expansion, the force on the satellite is expressed in terms of a time integral coupling the quadrupole component at time s to the correlation function $\mathcal{B}$ of the unperturbed background at time $(t-s)$. In this paper we will examine the physical effect that a force satisfying equation (9) can imprint on the motion of a satellite once we specify the nature of the underlying system, i.e., once we specify the interaction potential determining the properties of $\mathcal{B}$. In paper I, we derived the force acting on M within the impulse approximation. Here we wish to include the self-gravity of the stars. Because of the complexity of the mechanism, we consider the simplest but concrete model in which stars interact via a harmonic potential characterized by a proper frequency ω. We wish to gain insight into the main physical processes controlling the energy transfer between the satellite and the stellar system.

III. HARMONIC POTENTIAL

We consider the response of a spherical stellar background which is characterized by a one-particle Hamiltonian

$$H_0 = \frac{1}{2}mv^2 + \frac{1}{2}m\omega r^2, \tag{10}$$

where ω is the internal frequency of the stars and is independent of radius r. The corresponding one-particle distribution function, Gaussian in velocity space (eq. [9])

$$f^{\rm op} = \left(\frac{m\beta\omega}{2\pi}\right)^3 e^{-\beta H_0} \tag{11}$$

is defined so that

$$\int d_3\mathbf{r}\, d_3\mathbf{v} f^{\rm op} = 1. \tag{12}$$

In the harmonic potential orbits are degenerate since a unique frequency characterizes the motion. This is a simplification since the mean field potential of a collisionless stellar system in virial equilibrium allows, in general, for a continuum distribution of angular frequencies. The harmonic potential describes an external force field but despite this approximation we hope to capture the relevant characteristics of the complex physical process of binary decay.

In the harmonic potential the stars perform bound orbits around the center of symmetry with a random distribution of amplitudes and phases. The corresponding expression for the correlation function

$$\begin{aligned}\mathcal{B}(t-s) &=< v^x\, x(t-s)\, y\, y(t-s) > \\ &=< v^x\, x(t-s) >< y\, y(t-s) >\end{aligned} \tag{13}$$

simplifies considerably since the motions along orthogonal direction are uncorrelated in this potential (we denote the components of $\mathbf{r} = (x, y, z)$ and $\mathbf{v} = (v^x, v^y, v^z)$, for simplicity). Accordingly we find

$$\mathcal{B}(t-s) = \frac{\sin(2\omega(t-s))}{2(\beta m)^2\omega^3}. \tag{14}$$

Given $\mathcal{B}$ we can compute the back-reaction force [eq. (9)]: The motion of the satellite is therefore determined by the combined effect of the Keplerian force and of $\mathbf{F}_\Delta$. The system under study is simple enough that we are able to construct a set of ordinary differential equation describing the dynamics of the satellite. The calculation is self-consistent and we do not introduce any artificial or simplifying assumption on the motion of the satellite and on the magnitude of its velocity relative to the stellar dispersion velocity. Resonances that may cause secular changes in the orbital parameters of the satellite are thus implicitly present in the solution.

For this purpose we define the tensor

$$I^{bc}(t) = \int_{-\infty}^{t} ds\ \mathcal{B}(t-s) Q^{bc}(s) \tag{15}$$

satisfying the equation

$$\frac{d^2\, I^{bc}(t)}{dt^2} = -4\omega^2 I^{bc}(t) + \frac{1}{(m\beta\omega)^2} Q^{bc}(t), \tag{16}$$

derived from (14). The evolution of the satellite is computed coupling equation (16) to equation (1) along with (9)

$$\mu\frac{d^2 R^a}{dt^2} = -GMNm\frac{R^a}{|\mathbf{R}|^3} - [GM]^2 Nm^2\beta\, I^{bc} O^{abc}. \tag{17}$$

Equations (16) and (17) form a close set of ordinary differential equations for R^a and I^{bc} that can be solved after specifying the initial conditions.

Before integration, it is useful to introduce dimensionless variables that are defined adopting $< r^2 >^{1/2}$ and $1/\omega$ as units of length and time, respectively. According to this choice, equations (16-17) take the form

$$\frac{d^2\, I^{bc}}{dt^2} = -4I^{bc} + \frac{1}{9} Q^{bc} \tag{18}$$

$$\frac{d^2 R^a}{dt^2} = -\left(1 + \frac{M}{Nm}\right)\gamma_V \frac{R^a}{|\mathbf{R}|^3} - 3\frac{M}{Nm}\left(1 + \frac{M}{Nm}\right)\gamma_V^2\, \mathcal{F}^a \tag{19}$$

where the coefficient

$$\gamma_V = \frac{GNm}{< r^2 >^{1/2} < v^2 >} \tag{20}$$

gives the virial relation for the spherical galaxy in its unperturbed state: For the harmonic system, here considered, $\gamma_V = (4\pi/3)^{1/2}$.

If the keplerian motion is confined in the (x, y) plane, the components of the back-reaction force lie in the orbital plane as well, and the dimensionless vector $\mathcal{F}^a$ introduced in equation (19) reads

$$\mathcal{F}^x = -\frac{6}{R^5}(I^{xx}R^x + I^{xy}R^y) + \frac{15}{R^7}R^x \left[I^{xx}(R^x)^2 + I^{yy}(R^y)^2 + 2I^{xy}R^xR^y\right] \tag{21}$$

$$\mathcal{F}^y = -\frac{6}{R^5}(I^{yy}R^y + I^{xy}R^x) + \frac{15}{R^7}R^y \left[I^{xx}(R^x)^2 + I^{yy}(R^y)^2 + 2I^{xy}R^xR^y\right] \tag{22}$$

In (18-22) all variables are regarded as dimensionless and $\mathbf{R}$ is evaluated at current time t. The above equations are solved numerically. For the tensor I we impose, as initial condition, $I = 0$ with its derivative. At the onset of binary evolution, the satellite is either set into a *hyperbolic* or *bound* keplerian orbit. Hyperbolic orbits are parameterized by the values of the impact parameter b and by the velocity V. Elliptic orbits, at the onset of evolution, are uniquely specified by the semimajor axis a (or equivalently by the binding energy per unit mass E) and by the eccentricity e (or the angular momentum per unit mass J). The perturbation on a bound orbit is switch on a time $t_0 = 0$.

IV. CAPTURE CROSS SECTION

Because of the dissipative nature of the tidal force (paper I) a satellite of mass M can be *captured* from an *asymptotic free state*. Equations (18-22) are then solved numerically to determine, for a given mass ratio M/Nm, the maximum impact parameter b_c below which capture occurs, as a function V, the asymptotic velocity. Figure 1 shows b_c (in units of $< r^2 >^{1/2}$) against V (in units of $< v^2 >^{1/2} = 3\sigma$), for $M/Nm = 0.05$. We notice that b_c is a monotonic function of V; it increases without limit when $V \to 0$, but declines as $V \to \infty$ where $b_c \to 0$. In the high speed limit, we verified that the satellite trajectory can be equivalently computed using the force derived in paper I (eq. [52]).

For the case under consideration the critical impact parameter b_c drops below $< r^2 >^{1/2}$ when $V \sim 2< v^2 >^{1/2}$: In the real interaction the satellite would then travel through the stellar medium where *friction* intervenes to slow it down (see §5 and 6 of paper I): A merger will therefore inevitably ensue if the total energy loss by friction equals the kinetic energy at infinity, i.e., if

$$\frac{[GM]^2}{V^2}\rho_0 < r^2 >^{1/2} |\Delta\tilde{E}(b;\epsilon)| \sim \frac{1}{2}\mu V^2, \tag{23}$$

where we estimate the (dimensionless) total energy loss suffered by the satellite inside the stellar distribution $|\Delta\tilde{E}|$ using the expression derived in paper I for the case of a homogeneous cloud of radius $< r^2 >^{1/2}$ (see eq. [58] and [59] for the energy loss, plotted in Figure 5 of paper I). In the expression for $\Delta\tilde{E}$ which is a function of b, the minimum impact parameter ϵ is set equal to $\sim GM/V^2$ (since we are in the high speed limit); ρ_0 (in eq. [23]) is the stellar mean density approximated here as $\rho_0 \sim 3Nm/(4\pi < r^2 >^{3/2})$. Equation (23) establishes a link between b and the asymptotic velocity V; i.e., $b = b(V)$.

According to the above relation, there exists a limiting speed V_{max} (corresponding to $b = 0$), and in turn a maximum kinetic energy, above which the encounter does not end in a merger. When $J > 0$, the largest velocity that leads to a coalescence is smaller than V_{max}. It is useful to introduce the dimensionless variables $\hat{V} = V/< v^2 >^{1/2}$, the specific energy and angular momentum

$$\hat{E} \equiv \frac{2E}{\mu < v^2 >} = \hat{V}^2 \tag{24}$$

$$\hat{J} \equiv \frac{b}{L}\hat{V}; \tag{25}$$

in these units $\epsilon/< r^2 >^{1/2} \sim \gamma_V\, M/(Nm\hat{V})$. Equation (23) that applies to encounters with $b << r^2 >^{1/2}$, provides, equivalently, an implicit relation between $\hat{E}$ and the specific angular momentum $\hat{J} = \hat{J}(\hat{E})$.

Can determine the physical parameters necessary for the encounter to end in a final merger ? The diagram representing the possibilities for capture of a satellite as a function of the initial energy $\hat{E}$ and angular momentum $\hat{J}$ is given in Figure 2. The solid line gives $\hat{J}(\hat{E})$ resulting from equation (23) with $\epsilon \sim 0.05< r^2 >^{1/2}$; dots denote the values of $\hat{J}$ and $\hat{E}$ inferred from the numerical runs (as in Figure 1). Dots describe the condition for tidal capture in wide encounters for which b exceeds the virial radius $< r^2 >^{1/2}$. In the $(\hat{E}, \hat{J})$ plane, the condition for capture can be derived combining the two curves, i.e., joining the dots with the continuous line, appropriate for encounters with b smaller than the virial radius. An equivalent plot is reported in Binney and Tremaine (1987; page 455) illustrating the merger conditions obtained from N-body calculations of binary encounters between equal mass galaxies with internal structure.

$\hat{E}_{max} \equiv \hat{V}_{max}$ is an increasing function of the mass ratio M/Nm, and depends on ϵ, the "permitted size" of the satellite. The values of $\hat{E}_{max}$ cluster between 1 and 2.5 for mass ratios M/Nm in the interval (0.01,0.1). These are approximate estimates of the maximum kinetic energy since they are based on the simple homogenous model of paper I.

In exploring the orbital evolution of capture orbits we find that trapping evolves always into a merger, i.e., into a state with $R(t) \to 0$: no bound Keplerian orbits develop from asymptotic free states, as a consequence of tidal dissipation.

V. EVOLUTION OF BOUND ORBITS

In paper I, we have shown that in flybys orbital energy is transferred into the internal degrees of freedom of the galaxy. Along a *bound* orbit, do tides cause dissipation ? Or alternatively, do they only modify the gravitational field without causing any energy loss ?

5.1 Circularization and orbital decay

We here explore the evolution of a satellite moving initially on a Keplerian orbit with fixed semimajor axis a (expressed below in units of $< r^2 >^{1/2}$) but different eccentricity e. Figure 3 illustrates a collection of orbits with $a = 3$ and mass ratio $M/Nm = 0.1$. We find that for eccentricities $e > 0.5$, the satellite grazing the outskirts of the stellar distribution eventually suffers complete merger. When the satellite performs, in its motion, a number of cycles before plunge in, we find clear *evidence of circularization* of the orbit (see panel (a)). Only at high eccentricities, the coalescence proceeds so rapidly to prevent circularization, as shown in panel (b).

From our numerical inspection, we also find that a *merger* occurs when the pericentric distance

$$a_p = a(1 - e) \tag{26}$$

is close to a critical value

$$a_{p,crit} \sim 1.6 \tag{27}$$

Thus wide bound orbits, those with $a \gg 1$, are unstable orbits only when

$$e \gtrsim (1 - a_{p,crit}/a). \tag{28}$$

Condition (28) implies the existence of a limiting distance of closest approach: *Circular orbits* are *stable* unless $a \lesssim 1.6$. Panel (c) of Figure 3 depicts the orbital evolution of a satellite set initially on a nearly circular orbit ($e = 0.3$) at $a = 3$. The satellite maintains always at a distance from the galaxy and tides are not

efficient to extract orbital energy. The orbit displays precessional motion since the back-reaction force causes the potential to deviate from its Keplerian value (see panel (d) of Figure 3).

With decreasing mass ratio, the tidal acceleration (scaling as M/Nm) weakens in magnitude. Nevertheless, orbital decay occurs provided condition (28) (derived from the numerical analysis) is fulfilled. In Figure 4a and 4b, we track the orbital decay of a satellite with $M/Nm = 0.01,\ a = 3$ and different eccentricities. In this case, a larger number of orbital cycles is completed before final plunge thus increasing the timescale of tidal infall (compare with Figure 3a and 3b). Panel (c) and (d) of Figure 4 reports on the evolution of eccentric orbits with $a = 5$. For lighter satellites the rate of circularization per revolution is smaller; nevertheless they perform a larger number of cycles before accreting onto the primary. As a result, orbits with eccentricities $e \lesssim 0.7$ (approximately) tend to circularize before coalescence.

In exploring evolution of stable orbits, those not ending in a merger, we find that the tidal field on M induces only precessional motion.

5.2 Tidal drag and the role of resonances

Can we have a deeper understanding on the mechanisms of energy and angular momentum exchange for the system under study ? How our findings compare with those that can be derived using Weinberg's perturbative approach (1986; Tremaine & Weinberg 1984) ?

In Weinberg's derivation of the frictional torque experienced by a satellite orbiting within a host galaxy, the motion was constrained to remain circular, during secular evolution. The torque was then evaluated considering the momentum exchange to the stars in the limit of $\mathcal{N} \to \infty$, where $\mathcal{N}$ gives the number of orbital cycles experienced by the satellite.

To gain insight into the role of resonances, in our analysis, we compute accordingly the fractional energy loss $\delta E/E_o$ that the satellite would experience when constrained to move on a arbitrary circular orbit characterized by a rotational frequency Ω. This function is computed, within our model, solving for the equation of energy loss

$$\frac{dE}{dt} = \mathbf{V} \cdot \mathbf{F}_\Delta \tag{29}$$

using equations (19) (21) and (22): The tidal force is evaluated imposing circular motion on $\mathbf{R}$ and $\mathbf{V}$ (i.e., equation (18) is not included in the integration scheme). The resulting $\delta E/E_o$ can be regarded as a function of Ω and $\mathcal{N}$ since time integration can be halted after an arbitrary number of cycles.

After completion of one period $P = 2\pi/\Omega$, we find that the function $\delta E(\Omega)/E_o$, shown in Figure 5, displays a sequence of dips (spread over the entire frequency interval), a broad maximum about $\Omega \sim \omega$ followed by a decline. Dips (at which $\delta E/E_o = 0$) occur at frequencies $\Omega/\omega = 2, 2/3, 1/2, 2/5, 1/3...$, independently of the value of the satellite mass and of the radius of the circular orbit; only the magnitude of $\delta E/E_o$ depends on these parameters.

With increasing number of cycles, dips are found to sweep in the frequency space indicating that these features are non permanent, and the extent of the energy loss per cycle varies with time. This is a consequence of the memory effect which is intimately related to the properties of the correlation tensor. Remarkably, we find that only in the limit of $\mathcal{N} \to \infty$ a *resonance* at $\Omega = \omega$ develops: there, $\delta E/E_o$ attains its peak value, and vanishes elsewhere. The development of the resonance is already evident in our numerical runs after ~ 50 cycles.

Due to the simplicity of the model it is possible to derive an analytical expression for the rate of energy loss. When the satellite moves on a circular path of radius a, energy is transferred to the stellar system at a rate

$$\frac{dE}{dt} = -\left[GM\right]^2 Nm \frac{< v^2 >}{4a^6} \frac{\Omega}{\omega^3} \left[\frac{\sin 2(\omega-\Omega)t}{2(\omega-\Omega)} - \frac{\sin 2(\omega+\Omega)t}{2(\omega+\Omega)}\right]. \tag{30}$$

If we carry out integration over $\mathcal{N}$ cycles, the function δE vanishes for $\Omega \neq \omega$ when the following condition is fulfilled

$$\mathcal{M}\Omega = 2\mathcal{N}\omega, \tag{31}$$

which is consistent with the numerical finding. In the limit of $\mathcal{N} \to \infty$ a resonance develops

$$\frac{dE}{dt} = -\frac{\pi}{8}[GM]^2 Nm \frac{< v^2 >}{a^6} \frac{\Omega}{\omega^3} \left[\delta(\omega - \Omega) - \delta(\Omega + \omega)\right]. \tag{32}$$

One can furthermore prove that higher order harmonics develop when higher order terms in the multipole expansion of the force (eq.[2]) are included, in the limit $\mathcal{N} \to \infty$. Their strength however decays faster with increasing distance a. Equation (32) shows that after the decay of transient phenomena (related to the way in which the back-reaction force is turned on at $t = 0$) the instability against orbital decay ensues only if the satellite happens to move on the circular orbit having Keplerian frequency Ω_K in resonance with the stellar system

$$\Omega_K = \omega \tag{33}$$

Equation (33) thus defines the critical radius a_{crit} at which stability is lost along a circular orbit

$$a_{crit} = [\gamma_V (1 + M/Nm)]^{1/3}. \tag{34}$$

The value of a_{crit} depends weakly on the mass ratio; $a_{crit} = 1.3$ for $M/Nm = 0.01$.

We notice that only very light satellites would experience a tidal field so weak to maintain their motion circular over many cycles and for the stellar response to develop a resonance (eq. [32]). However, the process of orbital energy dissipation can not be solely interpreted as a resonance phenomenon since massive satellites (those with $M/Nm \gtrsim 0.01$) lose stability over a broader interval of orbital frequencies (as illustrated in Figure 5). Heavier satellites sweep fast across the resonance and the transient response of the galaxy guides evolution; stability is lost *near resonance*. The presence of dips, i.e., "negative interferences", is a new feature that can affect the orbital evolution of the satellite in the binary, delaying the process of tidal drag whenever the orbital frequency sweeps through a dip (see §6).

The transfer of angular momentum mimics that of energy. Confining the motion in the (x, y) plane, we find an analogous expression for the torque on the satellite which reads

$$\tau^z = -[GM]^2 Nm \frac{< v^2 >}{2a^6} \frac{1}{\omega^3} \left[\frac{\sin 2(\omega - \Omega)t}{2(\omega - \Omega)} - \frac{\sin 2(\omega + \Omega)t}{2(\omega + \Omega)}\right]. \tag{35}$$

5.3 Secular torque in a pinned galaxy

In this section we first derive an expression for the secular torque acting on the satellite, using TLR. In a second step, we compute the same quantity using Weinberg's formalism, as an independent test.

Weinberg's perturbative method (WPM hereafter) which adopts a factorized distribution function for the stars, provides the angular momentum loss in the case of a galaxy whose center is nailed down. The loss, computed in this case, contains a contribution, difficult to disentangle, resulting from the coordinated displacement of the stars due to linear momentum conservation.

We evaluated, within TLR, the torque, denoted with τ_{pin}, as a function of the number of cycles $\mathcal{N}$, for a satellite interacting with a primary having a pinned center of mass. In this circumstance, the back-reaction force is given by equation (16b) of paper I:

$$\mathbf{F}_\Delta(t) = -[GM]^2 Nm^2 \beta \int_{-\infty}^{t} ds \int d_3\mathbf{r}\, d_3\mathbf{v}\; f^{\rm op} v^a \frac{R^a(s) - r^a}{|\mathbf{R}(s) - \mathbf{r}|^3} \frac{\mathbf{R}(t) - \mathbf{r}(t-s)}{|\mathbf{R}(t) - \mathbf{r}(t-s)|^3}. \tag{36}$$

To lowest order in the multipole expansion (we retain the dipole and quadrupole terms), we compute the torque on the satellite. Assuming circular motion in the (x, y) plane, we find

$$\tau^z_{pin} = -\frac{[GM]^2 Nm}{2\omega a^4} \frac{\Omega}{2\pi\mathcal{N}\omega} \left(\frac{1}{(\Omega-\omega)^2} + \frac{1}{(\Omega+\omega)^2} \right) \left[1 - \cos\left(2\pi\mathcal{N}\frac{\omega}{\Omega} \right) \right]. \tag{37}$$

From equation (37) we again clearly infer the existence of the dips in correspondence of which the angular momentum loss vanishes (the energy loss mimics this behavior as well): Dips here occur when $\mathcal{N}\omega = \mathcal{M}\Omega$. The torque is a function of $\mathcal{N}$ and in the limit of $\mathcal{N} \to \infty$ (or $t \to \infty$) its expression converges to a delta function:

$$\tau^z_{pin} = -\frac{\pi}{2} \frac{[GM]^2 Nm}{\omega a^4} \left[\delta(\Omega-\omega) - \delta(\Omega+\omega) \right]. \tag{38}$$

In the limit of $t \to \infty$ we again infer the existence of the leading resonance.

We computed the secular torque within WPM for completeness. In Weinberg's work a scheme is presented for determining, given the expression of the unperturbed stellar potential (harmonic in the case of consideration), the "secular torque" experienced by the satellite, again, forced to move on a arbitrary circular orbit. We find that the expression of the torque calculated to lowest order in the multipole expansion is identical to equation (38).

Despite some similarities we find that the torque for a pinned galaxy differs in strength to the torque for a galaxy whose barycenter is free to move. In the interaction between the satellite and the galaxy with fixed center the angular momentum loss (of order G^2) scales as a^{-4}. In a binary, instead, the response involves higher order multipoles (from the coupling of quadrupolar and octupolar terms) and has accordingly a smaller amplitude scaling as a^{-6} (White 1983; Zaritsky & White 1988; Hernquist & Weinberg 1989).

VI. ORBITAL DECAY TIME

Numerical N-body simulations of binary mergers customary describe the evolution of galaxies of comparable mass and follow the onset of the merger process when the two members are just *near contact*. These restrictions arise since relaxation due to the finiteness of the system can introduce a number of spurious effects (see also Gelato, Chernoff & Wasserman 1992).

Using our simplified model, we can instead explore the process of orbital decay of a satellite in a binary before friction intervenes to accelerate and complete the merger process. Indeed, it is the time scale during the phase of detached binary the *longest* scale that determines the magnitude of the lifetime of the binary; τ_b depends on the energy, on the angular momentum and on the mass of the satellite M relative to Nm.

6.1 Binary decay time versus eccentricity

It is of interest to determine the characteristic time of binary orbital decay τ_b. This time scale is a function of the initial eccentricity, of the semimajor axis a, and on M/Nm, the ratio determining the strength of the tidal field. For this purpose we follow the dynamical evolution (until $R \to 0$) for a series of orbits having equal energy (i.e., equal semimajor axis a) but different angular momentum: In Figure 6 we give τ_b against e for $a = 2$ and $M/Nm = 0.1$ (dots).

We find that the time of coalescence clearly diminishes with increasing eccentricity. As $e \to 1$ the periastron distance a_p becomes smaller than $< r^2 >^{1/2}$ and the satellite experiences an intense tidal force suffering sudden energy loss (below $< r^2 >^{1/2}$ higher order terms in the multipole expansion become important and are neglected here as well as the drag by dynamical friction: both effect would speed up the process of orbital decay. Thus τ_b provide an upper limit).

The time of coalescence τ_b (expressed in units of the internal dynamical time ω^{-1}) varies from ~ 35 (for $e = 0.2$) to ~ 6 (for $e = 0.99$) corresponding to a time ratio (in the two limiting cases) of about ~ 6. This estimate is in agreement with the one resulting from numerical N-body simulation of sinking satellites in binaries that we are now performing (Mayer, Colpi & Governato 1997).

At eccentricities $e \sim (1-a_{p,crit}/a)$ the time becomes exceedingly long, since the satellite hits the stability limit. In real systems decay would proceed due to the energy exchange with loosely bound stars fulfilling condition (31).

As illustrated in Figure 6, we find, superposed to the clear monotonic rise with decreasing e, the existence of abrupt increases of τ_b: The satellite along these orbits performs many cycles with pericenter $a_p \gtrsim < r^2 >^{1/2}$ before sudden plunge in. The origin of these peaks can be attributed to the development of transient dips in the energy pattern $\delta E(\mathcal{N})/E_o$, delaying the infall. If for the same orbital parameters we diminish the extent of the tidal force by lowering the M/Nm ratio, the spikes in $\tau_b(e)$ appear over the whole range of eccentricities (as shown in Figure 6 for the case with $M/Nm = 0.05$ and $a = 2$).

In Figure 7 we plot τ_b as a function of the initial semimajor axis a for three values of the eccentricity $e = 0.1, 0.3, 0.5$, and $M/Nm = 0.1$. τ_b is found to be an increasing function of a since the tidal field displays a steep dependence on distance. Circular orbits with a in the interval (1.3,1.8) decay on a time scale which is increasing exponentially when $a \gtrsim 1.8$, above resonance.

6.2 Binary decay time versus M/Nm

Numerical simulations explore the process of orbital decay of spherical systems having comparable masses. Here, we can investigate a wider range to determine the dependence of τ_b on the mass ratio M/Nm. In Figure 8 we collect the results of integrations derived for circular orbits near resonance with a varying in the interval $(1.3, 1.7)$. The time τ_b corresponds to the instant at which $R = 1$. We find that it displays a power law dependence on M/Nm and a fit gives

$$\tau_b \propto \left(\frac{M}{Nm}\right)^{\alpha} \tag{39}$$

with a slope $\alpha \sim 0.4$ nearly independent of a. A similar recipe was introduced heuristically by Cole et al. (1994) in the description of the dynamical evolution of baryonic cores in massive dark matter haloes. We plot the two upper curves only above $M/Nm = 0.05$ since below this value the tidal field is weak and the two curves start displaying the erratic behaviour.

Figure 9a shows τ_b versus M/Nm for $e = 0.5$ and different initial semimajor axis $a \geq 2$. The lower curve gives the decay time for a satellite orbiting around the primary with a pericentric distance $a_p \sim 1$. In these grazing encounters the tidal field induces orbital decay on a time scale of ~ 5 dynamical times, regardless the value of M/Nm. Instead, in binaries with apocenter $a_p > 1$ the time of binary decay displays a dependence on M/Nm. At values $M/Nm \gtrsim 0.1$ the curve is monotonic and smooth with $\alpha \sim 0.3$. In Figure 9b we consider orbits with $e = 0.8$; the erratic behaviour is present whenever the initial orbits are wide (i.e., $a_p > 1$) and similarly to the case with $e = 0.5$, the time τ_b increases with decreasing mass ratio.

VII. CONCLUSIONS

The results presented in this paper are derived under the hypothesis that the satellite is interacting with a spherical system characterized by a unique proper frequency ω. In exploring evolution along circular orbits, we have shown that stability is lost when the Keplerian frequency of the relative orbit is comparable to the internal frequency of the stellar system; The process of energy exchange can thus be described in terms of a near resonance condition. This is a useful concept for interpreting the origin of the instability particularly for light satellites, those with $M/Nm \lesssim 0.01$. In this case, the energy exchange in each revolution is exceedingly small and the satellite performs many orbits around the companion galaxy: The response of the stellar system to the *periodic* perturbation thus appears as a sharp resonance at $\Omega_K = \omega$ in the energy diagram. For heavier satellites energy is transferred more effectively on a wider interval of orbital frequencies about ω. The response of the galaxy to the time dependent perturbation triggers orbital evolution before the mechanisms internal to the stellar system produce the resonance. Thus, heavier satellites sweep fast

through the unstable region of the frequence space. The presence of transient dips in the energy pattern (along circular orbits) suggests in addition that the transfer of orbital energy is a relatively complex process that produces the erratic behaviour in the time scale of binary decay. Along orbits of increasing eccentricity, stability is lost more rapidly than along circular orbits and sets in when the pericentric distance lies inside a critical radius corresponding to the Keplerian circular orbit with $\Omega_K \sim \omega$. This condition is equivalent to the one found by Aarseth & Fall (1980) in numerical N-body simulations.

In a real spherical galaxy, orbits are *non degenerate*; the stellar system is therefore characterized by a spectrum of internal frequencies N_ω. The leading resonance at $\Omega_K \sim \omega$ important for the instability of light satellites would thus be replaced by a superposition of resonances with the effect of destabilizing the binary over a wider interval of orbital energies. Stars at the periphery of the galaxy moving with orbital frequency lower than the mean would cause secular decay from wider orbits. The back-reaction force, in the harmonic model, is found to depend on the mass ratio M/Nm and on the coefficient γ_V expressing the virial condition of the equilibrium system. We expect that in a real galaxy the force will result from the incoherent superposition of the different monochromatic contributions:

$$F^a_\Delta \propto O^{abc} \int d\omega N_\omega \int ds\, \mathcal{B}_\omega(t-s) Q^{bc}(s). \tag{40}$$

Equation (9) may thus represent the contribution from a single frequency. We have demonstrated that the back-reaction force can be expressed in terms of a dynamical 4-point correlation function $\mathcal{B}$ of the unperturbed stellar system. As a next step we will attempt to compute the back-reaction force exploring the general properties of the correlation function $\mathcal{B}$ of non degenerate spherical systems with the aim at exploring the dependence of $\mathbf{F}_\Delta$ on the spectral distribution of stars and at determining the decay time τ_b as a function of the orbital parameters. We expect that the superposition of different spectral components will erase the discontinuities present in τ_b that will appear as a smooth function of the orbital parameters. This study is complementary to ongoing numerical investigations (Mayer, Colpi & Governato 1997) designed to explore the evolution of satellites accreting onto massive dark matter haloes. In these simulations the satellite is deformable and during binary evolution mass loss by tidal stripping (neglected in our formalism; Weinberg 1996) can become important. The comparison will prove useful for a deeper understanding of the process of orbital decay.

We thank G.Gyuk, M. Vietri and I. Wasserman for stimulating discussions, and G. Gyuk for a critical reading of the manuscript. This work was carried out with financial support from the Italian Ministero dell' Università e della Ricerca Scientifica e Tecnologica.

REFERENCES

Aarseth, S.J., & Fall, S.M. 1980, ApJ, 236,43
Bontekoe, Tj. R., & van Albada, T.S. 1987, MNRAS, 224,349
Cole, S., et al. 1994, MNRAS, 271, 781
Colpi, M., & Pallavicini, A. 1997, submitted to ApJ, (paper I)
Gelato, S., Chernoff, D.F., & Wasserman, I. 1992, 384, 15
Hernquist, L., & Weinberg, M.D. 1989, MNRAS, 238, 407
Lacey, C., & Cole, S. 1993, MNRAS, 262, 627
Lin, D.N.C., & Tremaine, S. 1983, ApJ, 264, 364
Lynden-Bell, D., & Kalnajs, A. 1972, MNRAS, 157, 1
Mayer, L., Colpi, M., Governato, F. 1997, in preparation
Navarro, J.F., Frenk, C.S., & White, S. 1994, 267, L1
Navarro, J.F., Frenk, C.S., & White, S. 1995, 275, 56
Tormen, G. 1997, to appear in MNRAS
Tremaine, S., & Weinberg, M.D. 1984, MNRAS, 209, 729
Weinberg, M.D. 1986, ApJ, 300, 93

Weinberg, M.D. 1996, astro-ph/9607099
White, S.D.M. 1983, ApJ, 274, 53
Zaritsky, D., & White, S.D.M. 1988, MNRAS, 235, 289

FIGURE CAPTION

Figure 1: Critical impact parameter b_c (in units of $< r^2 >^{1/2}$) below which capture occurs, against V (in units of $< v^2 >^{1/2}$), the satellite asymptotic velocity of the relative hyperbolic orbit; the mass ratio is $M/Nm = 0.05$.

Figure 2: Angular momentum $\hat{J}$ against energy $\hat{E}$ (in dimensionless units). *Dots* denote the relation derived from integration of equations (18-22); *Solid* line indicates the relation derived using equation (23) for $M/Nm = 0.05$ and $\epsilon/< r^2 >^{1/2} = 0.05$.

Figure 3: A collection of orbits in the plane (x, y); the semimajor axis (in units of $< r^2 >^{1/2}$) is $a = 3$ at the onset of evolution, and $M/Nm = 0.1$. The *dash-dotted* circle indicates the size of the primary galaxy. Distances are in units of $< r^2 >^{1/2}$. Panel (a) is for an initial eccentricity $e = 0.5$; (b) is for $e = 0.6$; (c) for $e = 0.3$ and (d) for $e = 0.4$.

Figure 4 : A collection of orbits in the plane (x, y) for a satellite with $M/Nm = 0.01$; the *dash-dotted* circle indicates the size of the primary galaxy. Distances are in units of $< r^2 >^{1/2}$. Panels (a) and (b) refer to orbits with initial $a = 3$ and $e = 0.5$ and 0.6, respectively. Panels (c) and (d) depict the evolution of orbits with $a = 5$ and $e = 0.8$ and 0.9, respectively. a is in units of $< r^2 >^{1/2}$.

Figure 5: $\delta E/E_o$ for $\mathcal{N} = 1$ as a function of Ω/ω.

Figure 6: Time scale of binary decay τ_b (in units of ω^{-1}) as a function of the initial eccentricity e for $a = 2$. *Dots* connected by a solid line refer to $M/Nm = 0.1$; *Squares* connected by a dash-dotted line refer to $N/Nm = 0.05$.

Figure 7: Dimensionless time τ_b as a function of semimajor axis a, for $M/Nm = 0.1$. *Triangles* correspond to $e = 0.5$; *Dots* correspond to $e = 0.3$ and *Squares* correspond to $e = 0.1$.

Figure 8: τ_b as a function of M/Nm, for orbits with $e = 0$. From bottom to top, the semimajor axis a (in units of $< r^2 >^{1/2}$) is equal to 1.3, 1.4, 1.5, 1.6, 1.7.

Figure 9: (9a) τ_b as a function of M/Nm, for orbits with $e = 0.5$. From bottom to top, the semimajor axis a (in units of $< r^2 >^{1/2}$) is equal to 2, 2.3, 2.5, 2.7.; (9b) τ_b as a function of M/Nm, for orbits with $e = 0.8$. From bottom to top, the semimajor axis a is equal to 5, 5.3, 5.5.

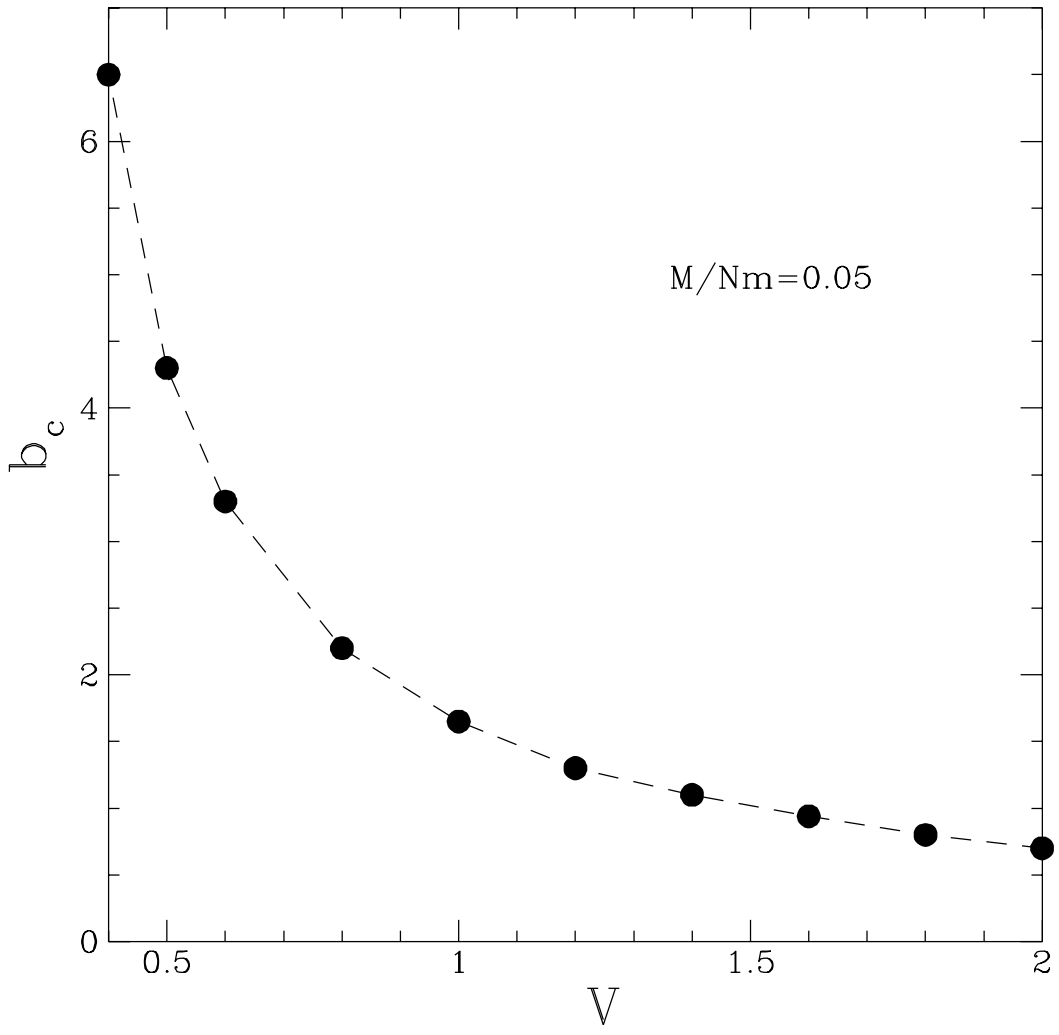
M/Nm=0.05
b_c
V
0
2
4
6
0.5
1
1.5
2

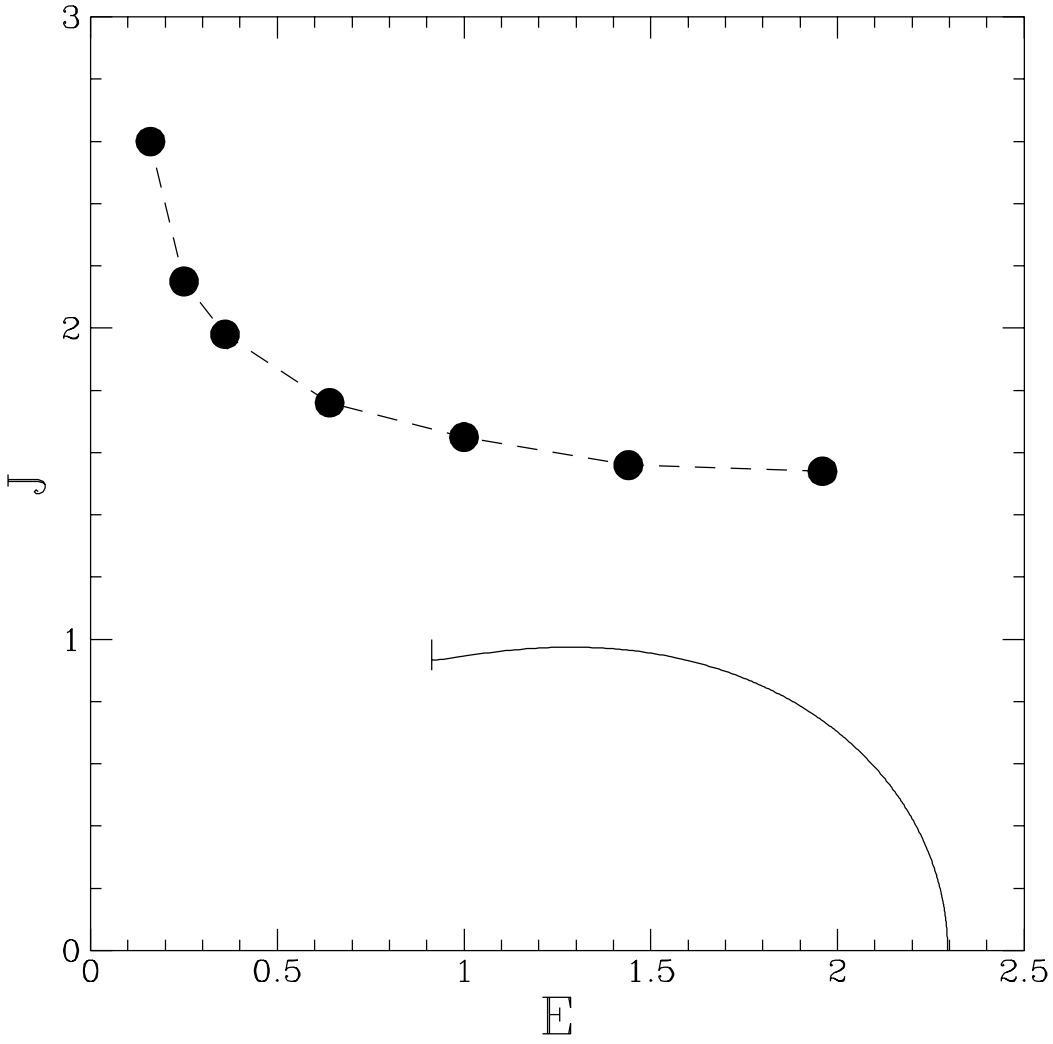
3
2
1
0
J
0
0.5
1
1.5
2
2.5
E

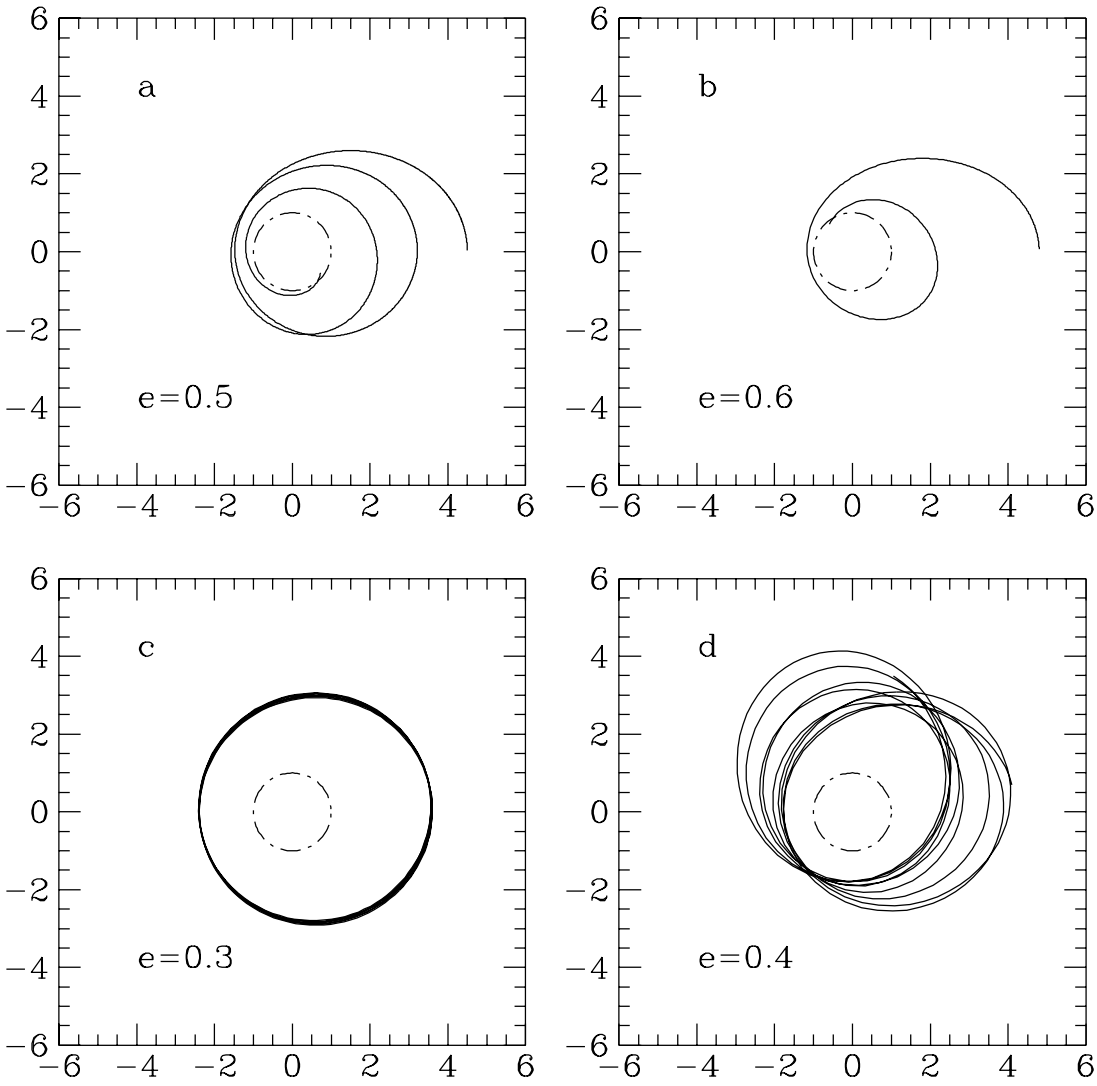
a
e=0.5
b
e=0.6
c
e=0.3
d
e=0.4
6
4
2
0
−2
−4
−6
−6 −4 −2 0 2 4 6

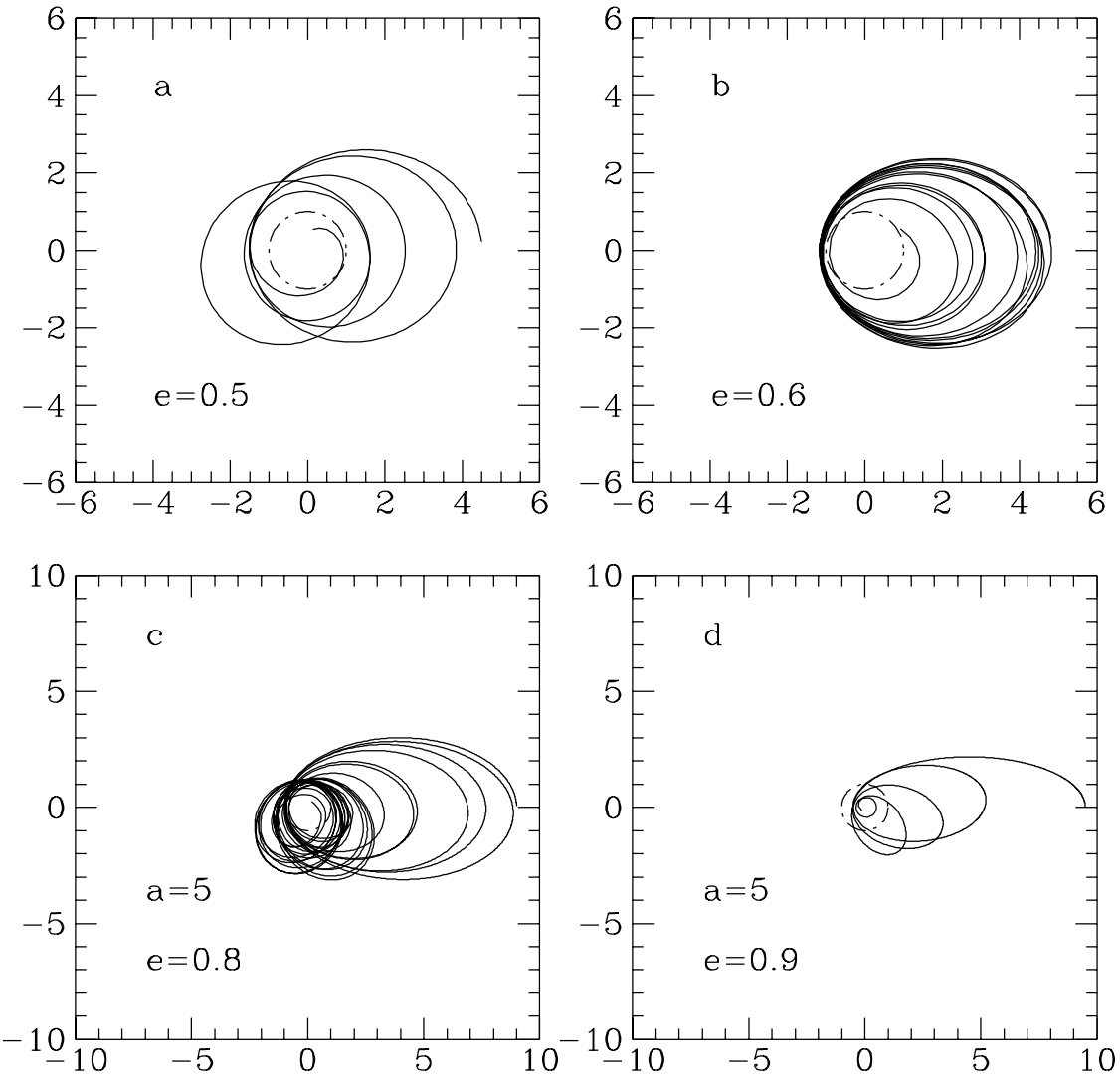
a
e=0.5
b
e=0.6
c
a=5
e=0.8
d
a=5
e=0.9

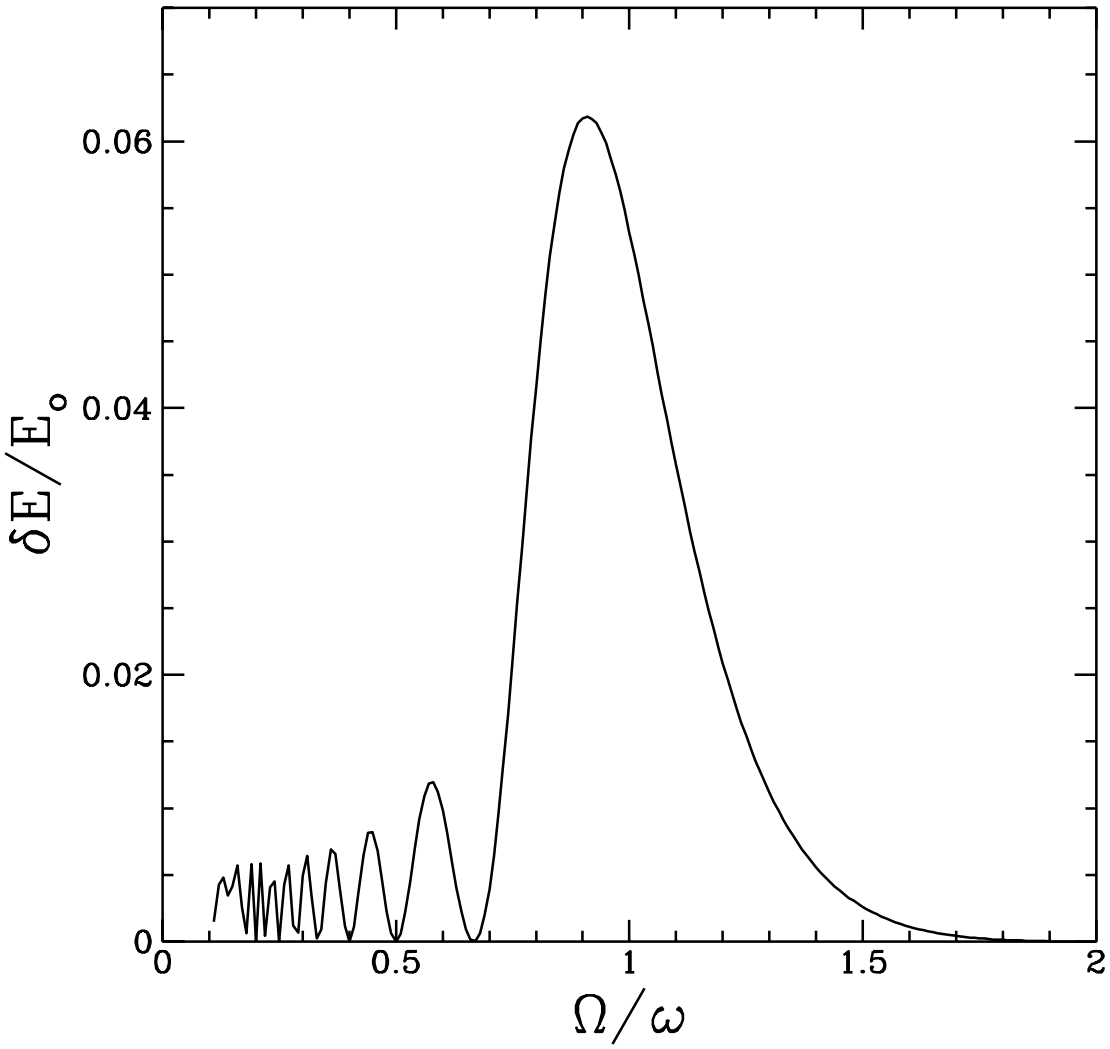
0.06
0.04
0.02
0
0
0.5
1
1.5
2
δE/E_o
Ω/ω

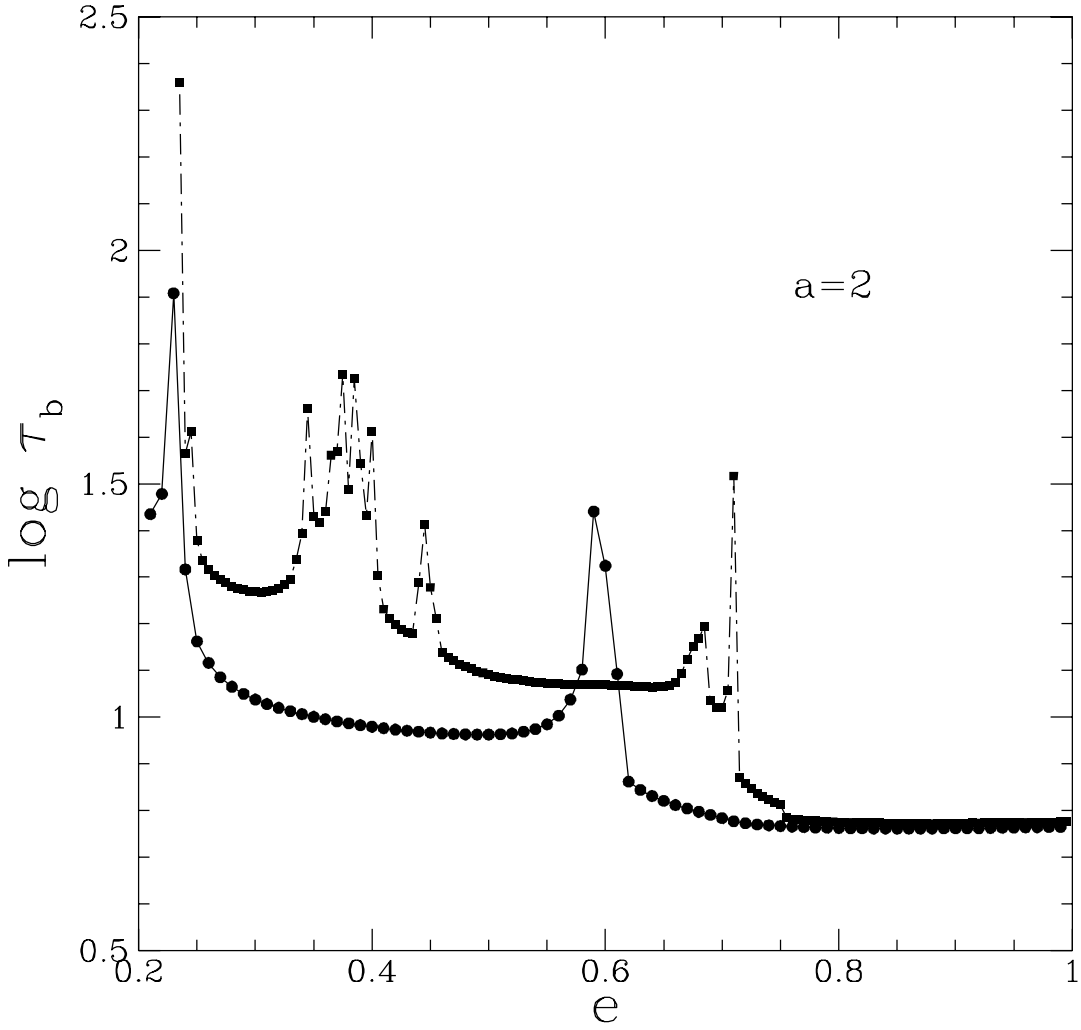
2.5
2
1.5
1
0.5
0.2
0.4
0.6
0.8
1
log τ_b
e
a=2

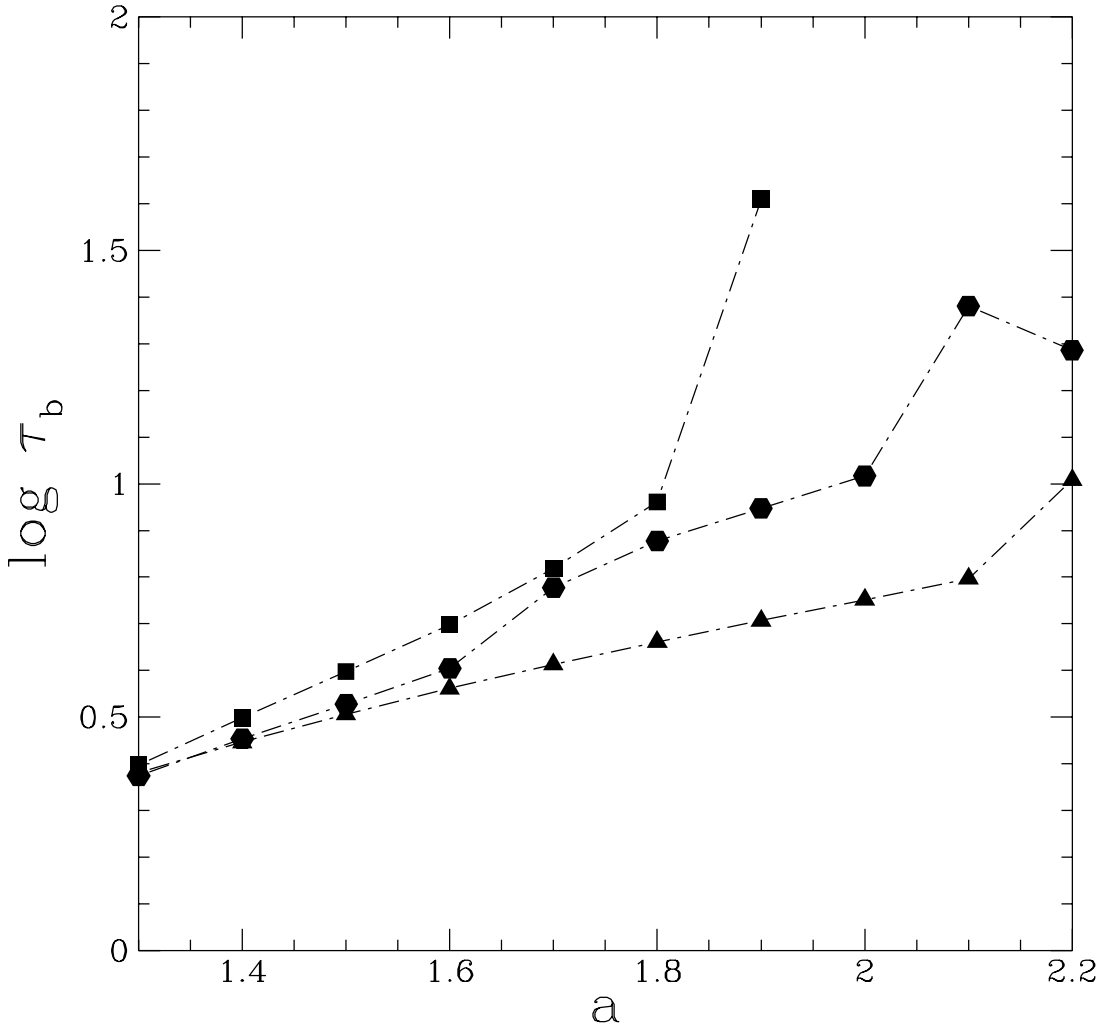
2
1.5
1
0.5
0
log τ_b
1.4
1.6
1.8
2
2.2
a

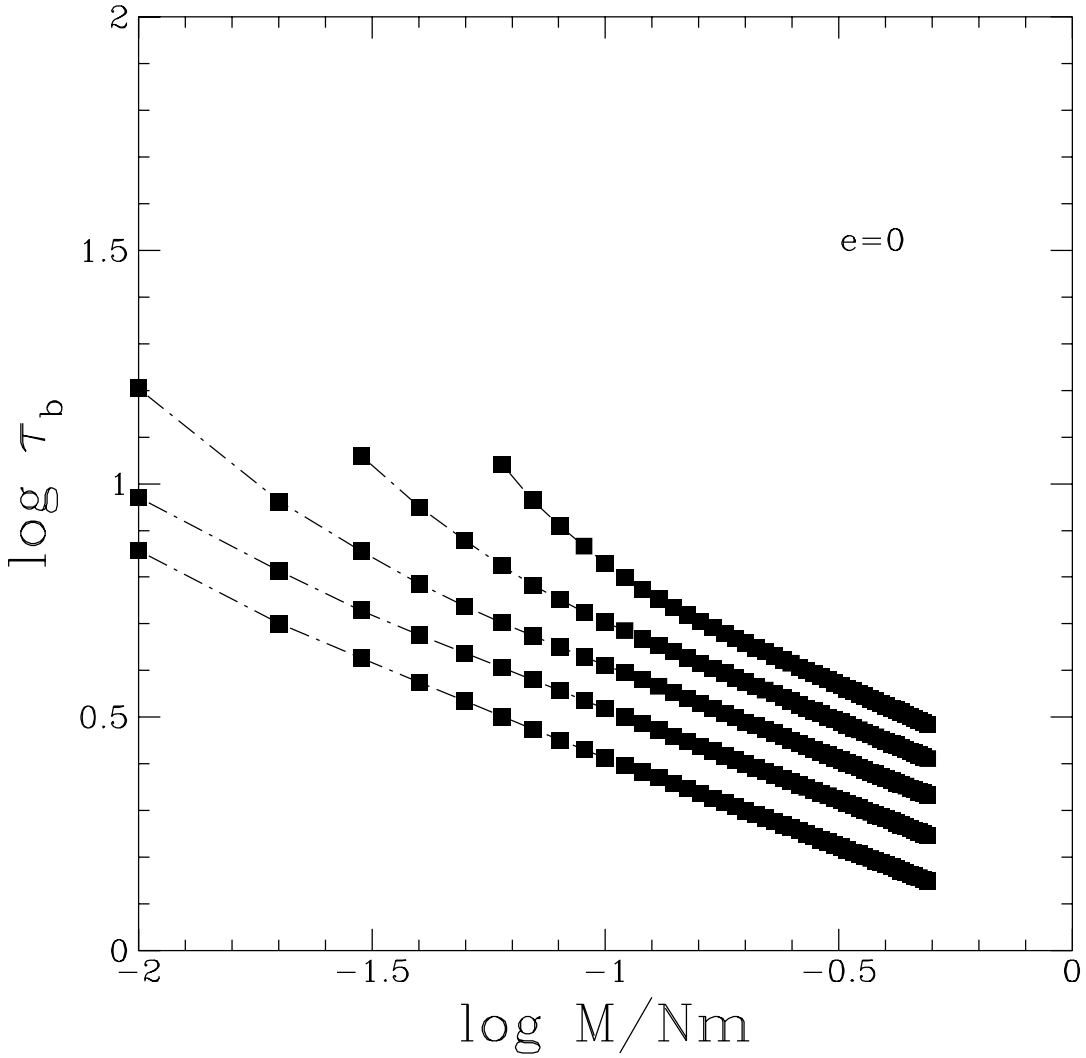
e=0
log τ_b
log M/Nm
2
1.5
1
0.5
0
−2
−1.5
−1
−0.5
0

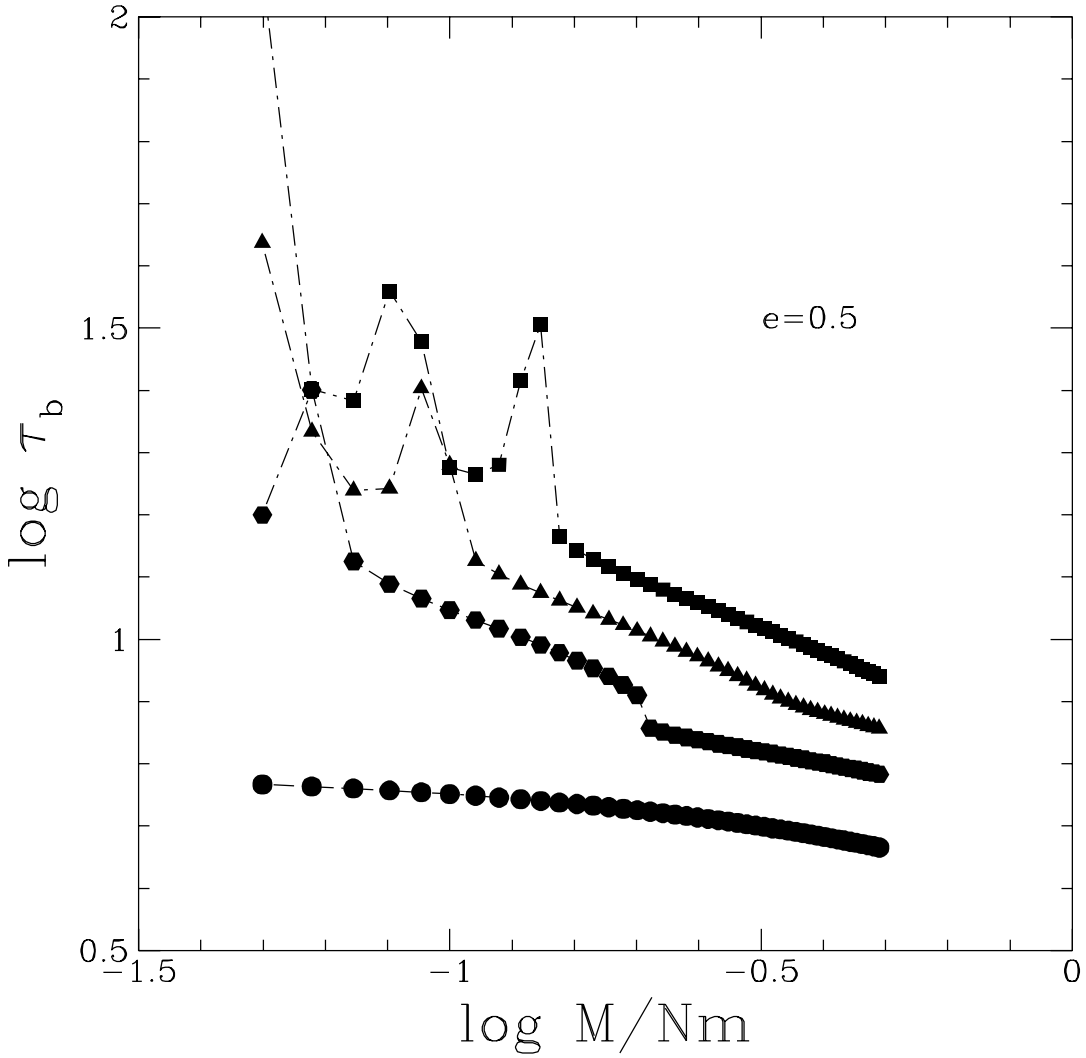
2
1.5
1
0.5
−1.5
−1
−0.5
0
log τ_b
log M/Nm
e=0.5

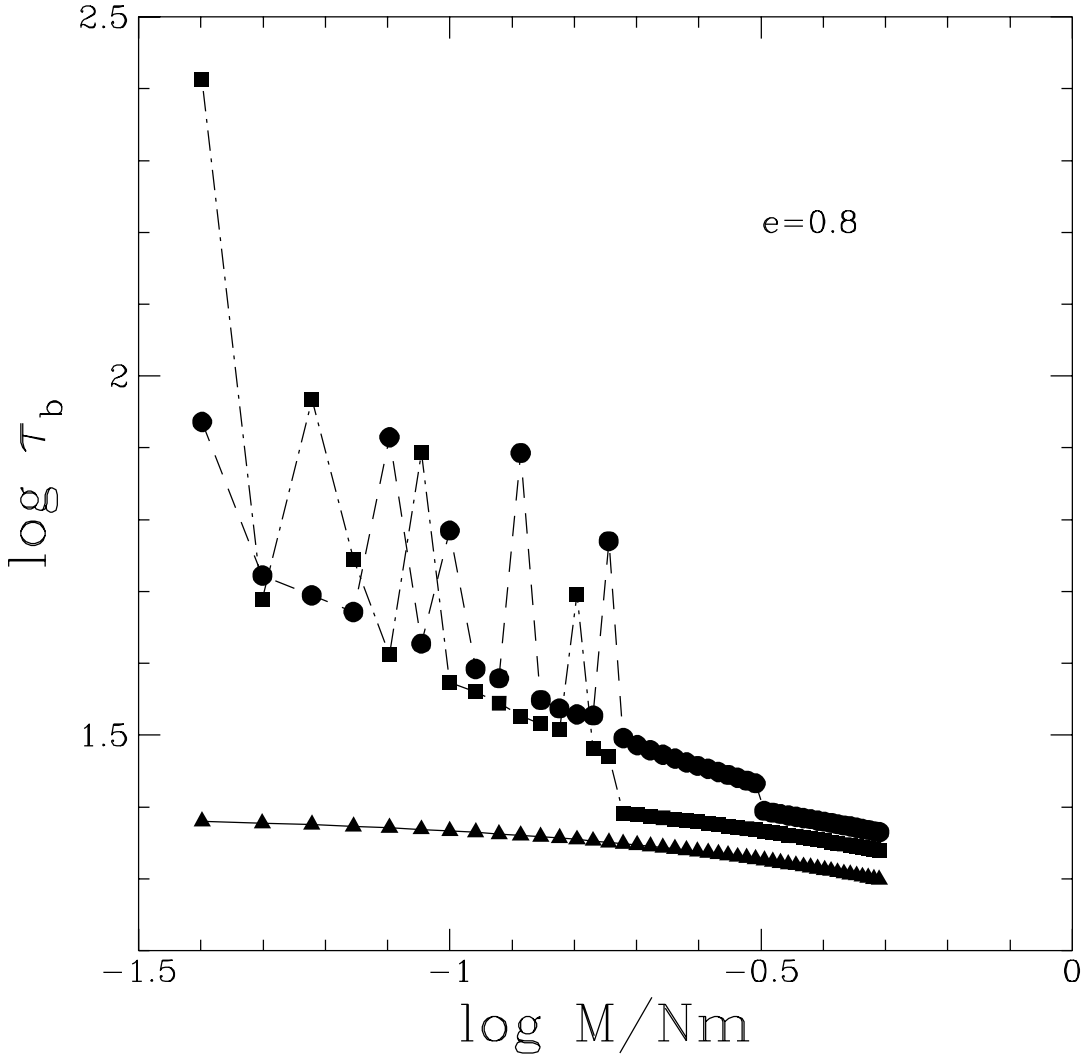
2.5
2
1.5
−1.5
−1
−0.5
0
log τ_b
log M/Nm
e=0.8